THE JOURNAL OF BIOLOGICAL CHEMISTRY VOL. 289, NO. 6, pp. 3677–3688, February 7, 2014

Vinculin Phosphorylation at Tyr^{1065} Regulates Vinculin Conformation and Tension Development in Airway Smooth Muscle Tissues*

Received for publication, August 13, 2013, and in revised form, December 3, 2013 Published, JBC Papers in Press, December 13, 2013, DOI 10.1074/jbc.M113.508077

Youliang Huang, Richard N. Day, and Susan J. Gunst[1]

From the Department of Cellular and Integrative Physiology, Indiana University School of Medicine, Indianapolis, Indiana 46202-5120

Background: Vinculin assumes a closed inactive or an open talin/actin-binding conformation. During airway smooth muscle contraction, vinculin undergoes Tyr^{1065} phosphorylation.
Results: Tyr^{1065} phosphorylation is required for vinculin conformation-sensitive FRET probes in smooth muscle to assume an open conformation and for tension generation.
Conclusion: Tyr^{1065} phosphorylation regulates the ligand-binding function of vinculin in airway smooth muscle.
Significance: Tyr^{1065} phosphorylation enables regulation of vinculin conformation by external stimuli.

Vinculin localizes to membrane adhesion junctions in smooth muscle tissues, where its head domain binds to talin and its tail domain binds to filamentous actin, thus linking actin filaments to the extracellular matrix. Vinculin can assume a closed conformation, in which the head and tail domains bind to each other and mask the binding sites for actin and talin, and an open activated conformation that exposes the binding sites for talin and actin. Acetylcholine stimulation of tracheal smooth muscle tissues induces the recruitment of vinculin to the cell membrane and its interaction with talin and actin, which is required for active tension development. Vinculin phosphorylation at Tyr^{1065} on its C terminus increases concurrently with tension development in tracheal smooth muscle tissues. In the present study, the role of vinculin phosphorylation at Tyr^{1065} in regulating the conformation and function of vinculin during airway smooth muscle contraction was evaluated. Vinculin constructs with point mutations at Tyr^{1065} (vinculin Y1065F and vinculin Y1065E) and vinculin conformation-sensitive FRET probes were expressed in smooth muscle tissues to determine how Tyr^{1065} phosphorylation affects smooth muscle contraction and the conformation and cellular functions of vinculin. The results show that vinculin phosphorylation at tyrosine 1065 is required for normal tension generation in airway smooth muscle during contractile stimulation and that Tyr^{1065} phosphorylation regulates the conformation and scaffolding activity of the vinculin molecule. We conclude that the phosphorylation of vinculin at tyrosine 1065 provides a mechanism for regulating the function of vinculin in airway smooth muscle in response to contractile stimulation.

The contractile stimulation of tracheal smooth muscle triggers a complex array of cytoskeletal events that are orchestrated by the protein complexes that localize to membrane adhesion junctions (adhesomes), where cytoskeletal proteins link actin filaments to the extracellular matrix. Pathways mediated by adhesome proteins collaborate with pathways initiated by G-protein-coupled receptors to mediate the assembly and activation of cytoskeletal signaling pathways that regulate the polymerization of a pool of actin, and to activate actomyosin cross-bridge cycling. Studies of a number of smooth muscle tissues have shown that cytoskeletal processes, including adhesome protein assembly and activation and actin polymerization, are required in addition to cross-bridge cycling to generate the development of active tension, and that contractile tension development is impaired when any of these processes are inhibited (1–10).

Vinculin and its muscle-specific isoform, metavinculin, are well documented constituents of adhesion junctions in smooth muscle cells and tissues (11, 12). Vinculin was first identified in smooth muscle tissues and non-muscle cells as an actin-binding protein that localizes to the adhesion junctions that form an interface between the termination of actin filaments within the cell and the extracellular matrix (12, 13). Vinculin binds directly to actin filaments and anchors them to transmembrane integrin proteins indirectly through its binding to talin and α-actinin, which are integrin-binding proteins that can also bind directly to filamentous actin (14–19). Although vinculin has traditionally been viewed as a stable constituent of adhesion junctions in smooth muscle tissues (20, 21), it is widely recognized to play a dynamic role in the growth and maturation of adhesion junctions during cell migration and traction in substrate adherent cells (22). Our studies have shown that vinculin plays an active role in tension generation in airway smooth muscle tissues during active contraction (10, 23). In these tissues, contractile stimulation triggers the recruitment of vinculin to the membrane and its assembly into membrane adhesomes that regulate actin polymerization (10, 23, 24).

The vinculin molecule consists of a globular head domain with four helical bundle domains connected by a flexible linker to a short tail domain consisting of an additional helical bundle

* This work was supported, in whole or in part, by National Institutes of Health Grants R01 HL29289 and HL074099 (to S. J. G.).
[1] To whom correspondence should be addressed: Dept. of Cellular and Integrative Physiology, Indiana University School of Medicine, 635 Barnhill Dr., Indianapolis, IN 46202. Tel.: 317-274-4108; E-mail: sgunst@iupui.edu.

(25, 26). The conformational state of the vinculin molecule can be reversibly regulated between an activated "open" state and an inactive "autoinhibited" state (14, 15, 18, 19, 25, 27). In the open state, binding sites for talin and α-actinin on the head domain of vinculin and binding sites for F-actin on the tail domain are exposed, enabling vinculin to form connections between the actin cytoskeleton and integrin adhesion complexes (14, 19, 26, 28). In its closed conformation, a high affinity intramolecular interaction between the head and tail domains of the vinculin molecule obstructs the binding sites on vinculin for talin and α-actinin on the head domain and prevents actin binding to the tail domain (14, 19, 25, 27).

The mechanisms for vinculin activation remain controversial. Although talin binding by itself has been proposed to be sufficient to cause vinculin activation (29, 30), most biochemical and structural analyses are consistent with the view that the activation of vinculin requires the simultaneous interaction of vinculin with at least two of its binding partners, actin and talin, which may promote the open conformation of vinculin by generating internal molecular stretching forces (25, 28, 31, 32). The interaction of vinculin with acidic phospholipids and α-actinin may also contribute to the conversion of vinculin to an open conformation (33–35). Mechanical forces exerted on cells may also promote stabilization of the activated open conformation of vinculin (36). Changes in the conformation of vinculin enable it to act as a molecular switch for connections between cytoskeletal actin filaments and membrane adhesion protein complexes during stimulation of the cell and thus regulate the transmission of mechanical forces between the cytoskeleton and the extracellular matrix during contraction, adhesion, and migration.

In airway smooth muscle tissues, contractile stimulation triggers the recruitment of vinculin to membrane adhesomes, where it binds to both talin and actin (10, 23). Molecular interventions that disrupt the recruitment of vinculin to the membrane or prevent its interaction with talin result in a marked reduction of tension development by the smooth muscle tissues in response to a contractile stimulus (10, 23). Thus, in smooth muscle tissues, the recruitment of vinculin to adhesion complexes and its conversion to an open conformation in which it can bind to talin and actin are critical for contraction and tension development.

The mechanisms by which external stimuli regulate the conformation and function of vinculin are unclear. *In vitro* studies as well as *in vivo* studies in several cell types have described both tyrosine and serine phosphorylation sites on the vinculin molecule (37, 38). There is evidence that phosphorylation at the Tyr^{1065} site near the C terminus of the tail domain affects cell traction and spreading and the dynamics of the incorporation of vinculin into focal adhesions (37, 39, 40). We previously found that vinculin undergoes phosphorylation at tyrosine 1065 concurrently with force development during the stimulation of tracheal smooth muscle tissues with acetylcholine and that the phosphorylation of vinculin at this site remains elevated for the duration of the contraction (10). Thus, vinculin phosphorylation might provide a mechanism by which its scaffolding function can be regulated.

In the present study, we evaluated the possibility that vinculin phosphorylation at Tyr^{1065} provides a mechanism for regulating the function of vinculin during smooth muscle contraction. We expressed vinculin constructs with Tyr^{1065} point mutations in smooth muscle tissues to alter the phosphorylation status of the vinculin and incorporated these point mutations into vinculin conformation-sensitive FRET probes to determine how phosphorylation at this site affects the conformation of vinculin. Our results demonstrate that vinculin phosphorylation at Tyr^{1065} is required for the normal tension generation in airway smooth muscle during contractile stimulation and that Tyr^{1065} phosphorylation regulates the conformation and scaffolding activity of the vinculin molecule. We conclude that the phosphorylation of vinculin at Tyr^{1065} provides a mechanism for regulating the function of vinculin in airway smooth muscle in response to external stimulation.

EXPERIMENTAL PROCEDURES

Reagents and Antibodies—Antibodies used were as follows: rabbit anti-vinculin (pY1065) phosphospecific Ab[2] (Invitrogen); talin (Sigma); actin clone AC-40 (Sigma); polyclonal EGFP (Abcam); polyclonal vinculin (against canine cardiac vinculin); and polyclonal myosin light chain, custom made by BABCO (Richmond, CA). Reagents included the Duolink *in situ* proximity ligation assay (PLA) kit and Duolink anti-mouse Plus, anti-rabbit Minus (Olink Bioscience, Uppsala, Sweden) and lysis and F-actin stabilization buffers (Cytoskeleton, Denver, CO). Plasmid vectors used were pEGFP-vinculin plasmids encoding full-length chicken vinculin (residues 1–1066) provided by Dr. Susan Craig (Johns Hopkins University, Baltimore, MD) (41); non-phosphorylatable vinculin Y1065F and phosphomimetic vinculin Y1065E, constructed by site mutation at Tyr^{1065} using a QuikChange II site-directed mutagenesis kit (Stratagene); and vinculin conformation-sensitive FRET probes, constructed as described below using plasmids pmCerulean3-N1. Plasmids encoding the Cerulean-5aa-Venus and the amber mutant Venus FRET probes were used as controls to validate the function of the vinculin FRET probes.

Preparation of Smooth Muscle Tissues and Measurement of Force—Mongrel dogs (20–25 kg) were euthanized in accordance with procedures approved by the Institutional Animal Care and Use Committee, Indiana University School of Medicine. A segment of the trachea was immediately removed and immersed in physiological saline solution. Smooth muscle strips (1.0 × 0.2–0.5 × 15 mm) were dissected free of connective and epithelial tissues, attached to force transducers, and maintained in a tissue bath in physiological saline solution at 37 °C for the measurement of contractile force. They were then subjected to repeated contractions and stretch to generate maximal isometric force.

Transfection of Smooth Muscle Tissues with Plasmids—Plasmids encoding recombinant vinculin proteins, and vinculin FRET probes were introduced into tracheal smooth muscle strips by the method of reversible permeabilization as described

[2] The abbreviations used are: Ab, antibody; PLA, proximity ligation assay; MLC, myosin light chain; ACh, acetylcholine; EGFP, enhanced green fluorescent protein; aa, amino acid(s).

previously (4, 23, 24, 42, 43). Tissues were incubated successively in each of the following solutions: Solution 1, which contained 10 mM EGTA, 5 mM Na_2ATP, 120 mM KCl, 2 mM $MgCl_2$, and 20 mM TES (at 4 °C, pH 7.1, 100% O_2 for 120 min); Solution 2, which contained 0.1 mM EGTA, 5 mM Na_2ATP, 120 mM KCl, 2 mM $MgCl_2$, 20 mM TES, and 10 μg of plasmids (at 4 °C, pH 7.1, 100% O_2 overnight); Solution 3, which contained 0.1 mM EGTA, 5 mM Na_2ATP, 120 mM KCl, 10 mM $MgCl_2$, and 20 mM TES (at 4 °C, pH 7.1, 100% O_2 for 30 min); and Solution 4, which contained 110 mM NaCl, 3.4 mM KCl, 0.8 mM $MgSO_4$, 25.8 mM $NaHCO_3$, 1.2 mM KH_2PO_4, and 5.6 mM dextrose (at 22 °C, pH 7.4, 95% O_2, 5% CO_2 for 60 min). After 30 min in Solution 4, $CaCl_2$ was added gradually to reach a final concentration of 2.4 mM. The strips were then incubated in a CO_2 incubator at 37 °C for 2 days in serum-free DMEM containing 5 mM Na_2ATP, 100 units/ml penicillin, 100 μg/ml streptomycin, and 10 μg/ml plasmids to allow for expression of the recombinant proteins. Sham-treated tissues were subjected to identical procedures except that no plasmids were included in Solution 2.

Immunoblot and Immunoprecipitation of Proteins—Frozen muscle tissues were pulverized, and proteins were extracted for electrophoresis or immunoprecipitation using methods described previously (4, 10). For immunoprecipitation of talin, muscle extracts were precleared at 4 °C with protein A/G UltraLink Resin, incubated with antibodies against talin, and separated by 8% SDS-PAGE. Western blotting of immunoprecipitates or muscle extracts was performed to quantitate proteins.

Myosin Light Chain Phosphorylation—Frozen muscle tissues were immersed in dry ice-precooled acetone containing 10% (w/v) trichloroacetic acid and 10 mM dithiothreitol. The proteins were extracted using an 8 M urea buffer. Phosphorylated and unphosphorylated MLCs were separated by glycerol-urea polyacrylamide gel electrophoresis, transferred to nitrocellulose, and then immunoblotted for MLC (2, 4, 44). MLC and phosphorylated MLC were visualized by ECL and digitally quantified using a Bio-Rad ChemiDoc XRS detection system. The ratio of phosphorylated MLC to total MLC was calculated for each sample.

Analysis of F-actin and G-actin—The relative proportions of F-actin and G-actin were analyzed in smooth muscle tissues by fractionation as described previously (10). The tracheal smooth muscle strips were homogenized in F-actin stabilization buffer. Supernatants of the protein extracts were collected after high speed centrifugation (G-actin fraction). The pellets were resuspended in 10 μM cytochalasin D and then incubated to depolymerize F-actin. The supernatant (G-actin) and pellet (F-actin) fractions were subjected to immunoblot analysis using actin antibody (Sigma). The ratios of F-actin to G-actin were quantified using a Bio-Rad ChemiDoc XRS digital detection system.

Cell Dissociation and EGFP Fluorescence Imaging of Live Cells—Smooth muscle cells were enzymatically dissociated from tracheal muscle strips, plated onto glass coverslips, and allowed to adhere for 10–30 min as described previously (4, 23). The effects of ACh stimulation on the localization of EGFP vinculin was evaluated in freshly dissociated smooth muscle cells using a Zeiss LSM 510 confocal microscope. Images of smooth muscle cells were analyzed for regional differences in fluorescence intensity of EGFP-vinculin proteins by quantifying the pixel intensity with a series of cross-sectional line scans along the entire length of each cell (4, 23). The area of the nucleus was excluded from the analysis. The ratio of pixel intensity between the cell periphery and the cell interior was computed for each line scan by calculating the ratio of the average maximum pixel intensity at the cell periphery to the average minimum pixel intensity in the cell interior. The ratios of pixel intensities between the cell periphery and the cell interior for all line scans performed on a given cell were averaged to obtain a single value for each cell.

In Situ Proximity Ligation Assay—In situ PLAs were performed to detect interactions between talin and vinculin (45). PLA yields a fluorescent signal (fluorescent spot) when the target proteins are localized within 40 nm of each other. Dissociated cells were fixed, permeabilized, and incubated with primary antibodies against talin and vinculin. A pair of oligonucleotide-labeled secondary antibodies (PLA probes) was targeted to primary antibodies for talin and vinculin. PLA probe hybridization, ligation, amplification, and detection media were administered according to the manufacturer's instructions. Randomly selected cells from both unstimulated and ACh-stimulated groups were analyzed for talin-vinculin interactions by counting PLA fluorescent spots using a Zeiss LSM510 confocal microscope. Duolink Images Tool software (Olink Bioscience, Uppsala, Sweden) was used to quantitate PLA signals.

Vinculin Conformation-sensitive FRET Probes—Vinculin FRET probes to detect the conformation of the vinculin molecule were constructed similarly to those described by Chen *et al.* (46). These probes were extensively validated by Chen *et al.* (46) to assure that changes in FRET emissions reflect changes in the conformation of the vinculin molecule. Vinculin cDNA encoding amino acids 1–1066 with spacer GGR (glycine-glycine-arginine) after aa 883 and spacer VDGT (valine-aspartic acid-glycine-threonine) after aa 1066 was inserted into pmCerulean3-N1 at HindIII/SalI sites to make pmCerulean3-N1-vinculin. VenusA206K with a NotI restriction site at each end was inserted into pmCerulean3-N1-vinculin to generate the pmCerulean3-N1-vinculin-Venus vinculin FRET probe (Fig. 1*A*). Vinculin FRET Y1065E and vinculin FRET Y1065F mutant probe constructs were made by replacing the WT tail fragment with tail fragments containing the indicated mutations.

When the vinculin conformation-sensitive FRET probe is in a closed conformation, the excited state energy of the donor Cerulean probe can be transferred to the acceptor Venus probe. This quenches the donor emission (470 nm), and there is sensitized emission from the acceptor at 530 nm, resulting in a low ratio of donor to acceptor emission (Fig. 1*B*). When vinculin is in an open conformation, the probes are spatially separated, preventing energy transfer and allowing maximum donor Cerulean probe emission at 470 nm, causing an increase in the ratio of donor to acceptor emission (Fig. 1*B*).

Vinculin amber mutants were constructed to confirm that fluorescence measurements at 530 nm resulted from energy transfer between vinculin Cerulean and Venus probes (Fig. 1*B*). Amber is a non-fluorescent form of Venus with a cysteine substitution at tyrosine 67 (Y67C mutant Venus) (47). The amber

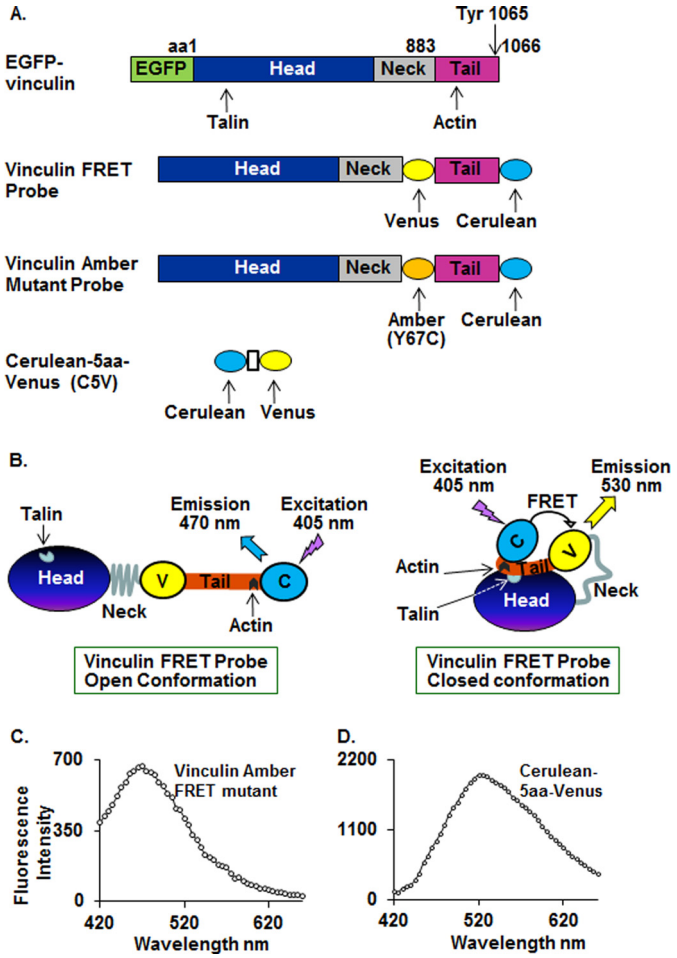

FIGURE 1. **Vinculin constructs used in these studies.** *A*, domain structure of EGFP-vinculin proteins, vinculin conformation-sensitive FRET probes, amber mutant, and Cerulean-5aa-Venus FRET probes. *B*, vinculin FRET probes in open and closed conformation. When vinculin is in an open conformation, there is maximum Cerulean probe emission at 470 nm. When vinculin assumes a closed conformation, Cerulean donor emission at 470 nm is quenched, and emission from the Venus acceptor at 530 nm is increased. *C*, emission spectrum of vinculin amber FRET mutant probe from a dissociated smooth muscle cell. Excitation at 405 nm on vinculin amber FRET mutant probe results in emission at 470 nm. *D*, emission spectrum of Cerulean-5aa-Venus FRET probe (*C5V*) from a dissociated smooth muscle cell. Excitation of Cerulean-5aa-Venus at 405 nm results in emission at 530 nm.

mutant folds correctly but is not able to act as FRET acceptor and can thus serve to verify that emission at 530 nm results from energy transfer from the donor probe. Vinculin amber mutants were constructed by replacing WT Venus with amber at the NotI site. Vinculin amber mutants were expressed in tracheal smooth muscle tissues as described above. Cells were dissociated from the tissues, and fluorescence emissions were analyzed. Excitation at 405 nm resulted in emission at 470 nm from the Cerulean probe, but no emission was detected at 530 nm, confirming that emissions at 530 nm are caused by energy transfer between the Cerulean and Venus probes (Fig. 1*C*).

Cerulean-5aa-Venus, a Cerulean-Venus pair that emits at 530 nm in response to excitation at 405 nm, was expressed in smooth muscle tissues as a positive control to confirm that FRET between Cerulean and Venus can be detected in cells dissociated from the muscle tissues. A strong FRET signal was detected at 530 nm in cells excited at 405 nm (Fig. 1*D*).

Analysis of Conformation-sensitive Vinculin Fluorescence Emissions in Tissues and Cells—Tracheal smooth muscle tissues expressing vinculin conformation-sensitive FRET probes were stimulated with ACh or left unstimulated before freezing. Emissions from vinculin conformation-sensitive FRET probes were analyzed in protein extracts from frozen smooth muscle tissues. Fluorescence emissions at 470 nm (donor emission) and 530 nm (acceptor emission) from each sample were obtained after excitation at 405 nm using a MicroSpectrometer (SpectraMax M2, Molecular Devices). The ratio of donor emission/acceptor emission was used to evaluate the FRET in each muscle tissue.

Live smooth muscle cells were dissociated from tissues expressing vinculin conformation-sensitive FRET probes, and fluorescence emissions were analyzed using an Olympus FV1000-MPE Spectral Confocal Microscope. An excitation wavelength of 405 nm was used, and the emission spectrum from 420 to 660 nm was recorded. The ratio of donor emission/acceptor emission at 470 and 530 nm was calculated for each cell.

Emissions from vinculin FRET biosensor probes at the membrane and in the cytoplasmic interior of the cell were calculated in six 1-μm^2 regions along the membrane and six 1-μm^2 regions in the cytoplasm of each cell. The ratios of donor emission/acceptor emission at the membrane and in the cytoplasm were calculated by separately averaging the donor/acceptor emission ratios for submembranous and cytoplasmic regions, avoiding the region of the nucleus (see Fig. 9*A*).

RESULTS

Expression of the Nonphosphorylatable Vinculin Mutant Y1065F Suppresses Endogenous Vinculin Phosphorylation at Tyr[1065] (Fig. 2)—Tracheal smooth muscle tissues were transfected with EGFP plasmids encoding WT vinculin, the nonphosphorylatable vinculin mutant Y1065F, or the phosphorylation mimetic Y1065E, or they were sham-treated. The expression of recombinant vinculin was confirmed by imaging EGFP fluorescence in live cells freshly dissociated from transfected smooth muscle tissues. Approximately 90% of dissociated cells expressed recombinant vinculin (data not shown).

Vinculin phosphorylation at Tyr^{1065} was evaluated in extracts from muscles treated with plasmids encoding vinculin Y1065F, Y1065E, and WT vinculin and in sham-treated muscles (Fig. 2*A*). The anti-vinculin antibody detects two isoforms of vinculin in extracts from the smooth muscle tissues, vinculin (116 kDa) and metavinculin (145 kDa), resulting in two bands on the immunoblot. Because EGFP recombinant vinculin migrates coincidentally with metavinculin, it cannot be distinguished from endogenous metavinculin using vinculin antibodies. However, we confirmed the expression of the recombinant EGFP vinculin proteins using anti-EGFP antibody (Fig. 2*A*).

Stimulation with ACh caused a significant increase in the phosphorylation of vinculin and metavinculin at Tyr^{1065} in sham-treated, vinculin WT-treated, and Y1065E-treated tissues, but the increase in vinculin/metavinculin phosphorylation was significantly inhibited in tissues expressing the nonphosphorylatable vinculin Y1065F (Fig. 2*B*) ($n = 7$, $p < 0.05$). No significant differences in the phosphorylation level of vin-

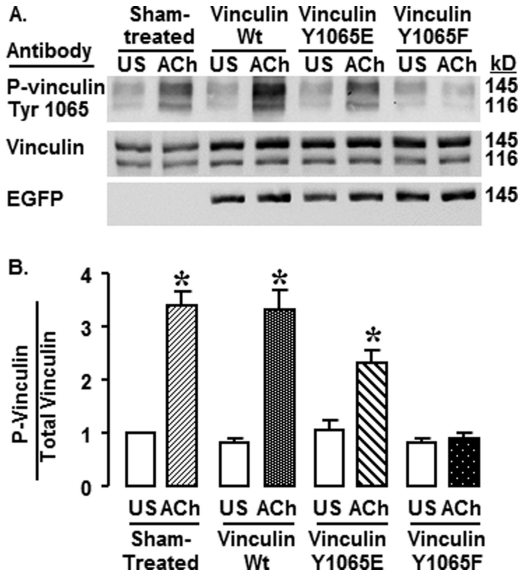

FIGURE 2. **Expression of Y1065F inhibits vinculin phosphorylation at Tyr[1065] in response to ACh.** *A*, immunoblots against phosphovinculin (pY1065), vinculin, and EGFP in protein extracts from unstimulated (*US*) and ACh-stimulated tissues that were sham-treated or expressing WT vinculin, vinculin Y1065E, or vinculin Y1065F. Vinculin Ab reacts with both vinculin (116 kDa) and metavinculin (145 kDa). The recombinant EGFP vinculin proteins have a similar mobility to metavinculin (145 kDa). Vinculin phosphorylation increased in ACh-stimulated tissues from Sham-treated, WT-transfected, and Y1065E-transfected tissues but not in those from Y1065F-transfected tissues. *B*, mean ratios of phosphovinculin normalized to total vinculin/metavinculin from each tissue. The phosphovinculin in ACh-stimulated tissues from sham-treated tissues and tissues expressing WT and Y1065E was significantly higher than that in unstimulated tissues; there was no significant difference between unstimulated and ACh-stimulated tissues in the Y1065F-treated group. Shown are means ± S.E. (*error bars*). *, significant difference between ACh and unstimulated tissues ($n = 7$, $p < 0.05$).

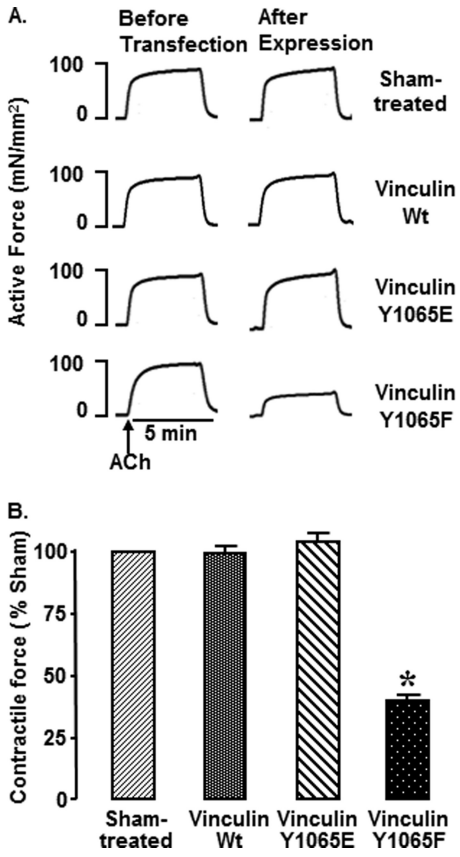

FIGURE 3. **Non-phosphorylatable vinculin Y1065F inhibits tension development in response to ACh.** *A*, representative isometric contractions in response to ACh stimulation in four muscles from one experiment. Contractions were measured before transfection of tissues with plasmids encoding vinculin Y1065F or Y1065E or WT vinculin and after 2 days of incubation for expression of recombinant proteins. Contractile force in response to ACh stimulation was dramatically inhibited in tissues treated with vinculin Y1065F ($n = 37$), but the force was not depressed in sham-treated ($n = 26$), vinculin Y1065E-expressing ($n = 26$), or WT vinculin-expressing ($n = 15$) tissues. *B*, mean ± S.E. (*error bars*) of force in response to 10^{-5} M ACh quantified as percentage force in sham-treated tissues. *, significant difference from sham-treated tissues ($p < 0.05$).

culin on Tyr[1065] were detected in unstimulated tissues. The level of vinculin phosphorylation in tissues expressing vinculin Y1065E appears lower than that in tissues expressing WT vinculin because phosphomimetic vinculin Y1065E does not react with the phosphospecific vinculin Y1065 Ab. In the vinculin Y1065E-expressing tissues, the antibody reacts only with endogenous Tyr[1065]-phosphorylated vinculin/metavinculin.

Inhibition of Vinculin Phosphorylation Inhibits Force Development in Smooth Muscle Tissues (Fig. 3)—Contractile force in response to stimulation with ACh was measured in tracheal muscle tissues before and after expression of the recombinant vinculin Y1065F, Y1065E, and WT vinculin and in sham-treated muscles. Expression of Y1065F decreased contractile force to 37 ± 3% of that in sham-treated tissues ($p < 0.05$). Expression of vinculin WT or Y1065E did not significantly affect contractile force.

Vinculin Phosphorylation Is Required for Actin Polymerization in Response to Contractile Stimulation with ACh (Fig. 4)—Phosphorylation of MLC is critical for the activation of actomyosin cross-bridge cycling and tension development in smooth muscle. MLC phosphorylation in response to ACh was compared in sham-treated muscle tissues and in muscle tissues expressing vinculin WT, Y1065E, or Y1065F (Fig. 4, *A* and *B*). The amount of MLC phosphorylation was not significantly different among any of the treatment groups ($p > 0.05$), although contractile force in the Y1065F-treated tissues was significantly depressed to 30 ± 3% of that in the sham-treated tissues (data not shown). This indicates that the inhibitory effect of Y1065F on contraction is not due to the disruption of pathways that regulate MLC phosphorylation.

The polymerization of a small pool of actin is required for contraction and force development in tracheal smooth muscle tissues, and the pathways that regulate actin polymerization are distinct from those that regulate MLC phosphorylation (7). We evaluated the effect of inhibiting vinculin phosphorylation at Tyr[1065] on ACh-induced actin polymerization in tracheal muscle tissues by determining the ratio of F-actin to G-actin in extracts from unstimulated and stimulated muscle tissues that had been transfected with vinculin WT, Y1065E, or Y1065F or were sham-treated (Fig. 4*C*). ACh stimulation significantly increased the F-actin/G-actin ratio in sham-treated, vinculin WT-treated, and vinculin Y1065E-treated tissues; however, expression of the Y1065F mutant significantly inhibited the ACh-stimulated increase in the F-actin/G-actin ratio ($p < 0.05$). In unstimulated muscles, the ratios of F-actin/G-actin were not significantly different among the four treatment groups.

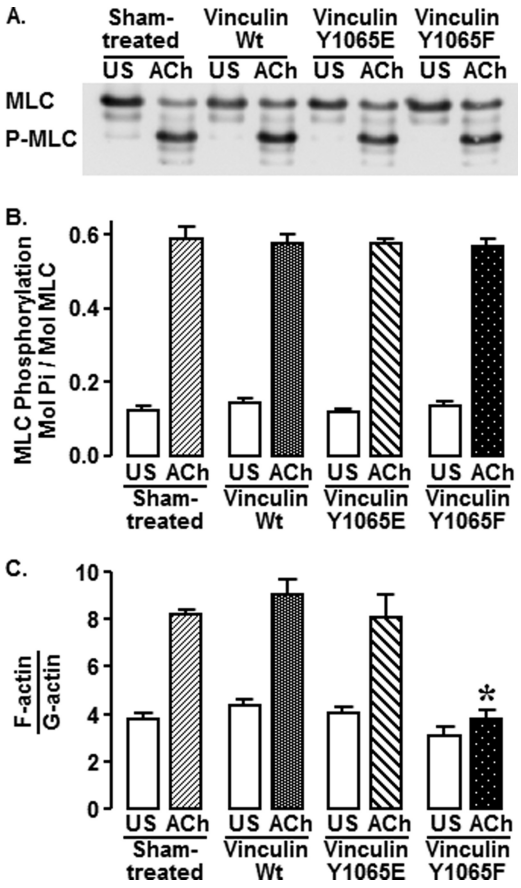

FIGURE 4. **Vinculin phosphorylation is required for ACh-stimulated actin polymerization but not for MLC phosphorylation.** Muscle tissues from sham-treated tissues and tissues expressing vinculin WT, Y1065E, or Y1065F were stimulated with 10^{-4} M ACh for 5 min or left unstimulated (*US*). *A*, immunoblot against MLC shows similar levels of MLC phosphorylation in tissues regardless of the expression of vinculin mutants. Phosphorylated and unphosphorylated MLC can be distinguished after urea gel electrophoresis. *B*, MLC phosphorylation was not significantly different among tissues subjected to different treatments ($n = 4$, $p < 0.05$). *C*, expression of Y1065F in smooth muscle tissues significantly inhibits the increase in the F-actin/G-actin ratio in response to ACh stimulation ($n = 4$, $p < 0.05$). Shown are means ± S.E. (*error bars*). *, significant difference from sham-treated tissues ($p < 0.05$).

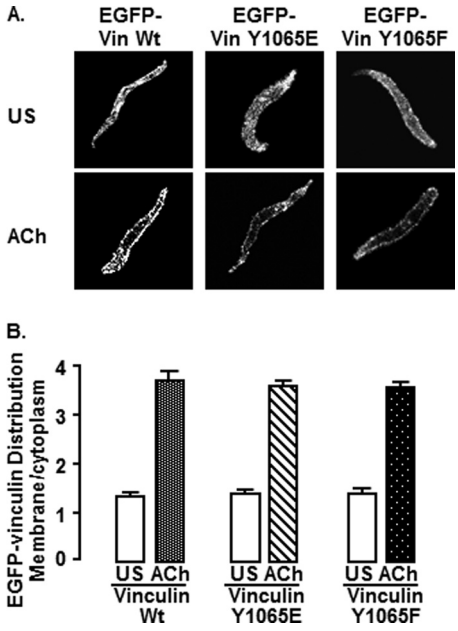

FIGURE 5. **Vinculin phosphorylation at Tyr[1065] does not affect the recruitment of vinculin to the membrane in response to ACh.** *A*, freshly dissociated smooth muscle cells from tissues expressing EGFP vinculin WT (unstimulated (*US*), $n = 17$; ACh, $n = 5$), vinculin Y1065E (unstimulated, $n = 25$; ACh, $n = 17$), or vinculin Y1065F (unstimulated, $n = 28$; ACh, $n = 14$) were plated onto coverslips and stimulated with 10^{-4} m ACh or left unstimulated. The localization of EGFP-vinculin was visualized in live cells by confocal microscopy. EGFP-vinculin WT, EGFP-vinculin Y1065E, and EGFP-vinculin Y1065F localized throughout the cytoplasm in unstimulated cells and were more heavily concentrated at the cell membrane in ACh-stimulated cells. *B*, mean ratios of pixel intensity between the cell membrane and cytoplasm. The membrane/cytoplasm ratio was significantly higher in ACh-stimulated cells from all recombinant vinculin treatment groups ($p > 0.05$). The localization of mutant and wild type vinculin EGFP-vinculin proteins did not differ significantly among different recombinant vinculin treatment groups. *Error bars*, S.E.

ACh Stimulates the Recruitment of EGFP Vinculin to the Membrane of Live Smooth Muscle Cells Independently of Its Phosphorylation State at Tyr[1065] (Fig. 5)—Vinculin is recruited to the submembranous cortex of tracheal smooth muscle cells in response to stimulation with ACh (10, 23). The effect of vinculin phosphorylation at Tyr^{1065} on the recruitment of EGFP-vinculin to the membrane in response to ACh was evaluated in live cells freshly dissociated from tissues expressing EGFP-vinculin Y1065E, Y1065F, or WT.

Stimulation with ACh significantly increased the ratio of membrane/cytoplasmic EGFP-vinculin in cells expressing WT vinculin, vinculin Y1065E, and vinculin Y1065F ($p < 0.05$) (Fig. 5, *A* and *B*). The ratio of membrane to cytoplasmic EGFP vinculin in unstimulated or ACh-stimulated cells was not significantly different in cells treated with WT vinculin, vinculin Y1065E, or vinculin Y1065F ($p > 0.05$). The localization of EGFP-vinculin was similar to that of endogenous vinculin as detected by immunofluorescence under both stimulated and unstimulated conditions (data not shown). Thus, the phosphorylation status of vinculin did not affect its recruitment to the smooth muscle cell membrane during contractile stimulation.

Inhibition of Vinculin Phosphorylation Prevents the Interaction of Vinculin with Talin in Tissues Stimulated by ACh (Figs. 6 and 7)—The binding of vinculin to talin and actin is essential for an open activated vinculin conformation that enables its scaffolding function within the adhesome (28).

We evaluated the effect of vinculin phosphorylation on the interaction of vinculin with talin in extracts of muscle tissues using co-immunoprecipitation analysis. Muscle tissues expressing vinculin WT, Y1065E, or Y1065F or sham-treated muscles were stimulated with ACh for 5 min or left unstimulated. Talin was immunoprecipitated from muscle extracts, and the precipitates were immunoblotted for vinculin, talin, and EGFP (Fig. 6*A*). In sham-treated, vinculin WT-treated, or vinculin Y1065E-treated muscles, the amount of vinculin that co-immunoprecipitated with talin was significantly higher in ACh-stimulated than in unstimulated muscles ($p < 0.05$) (Fig. 6*B*). In contrast, ACh stimulation did not increase the amount of vinculin that co-precipitated with talin in muscles expressing vinculin Y1065F, indicating that expression of Y1065F significantly inhibits the interaction of vinculin and talin induced by ACh stimulation (Fig. 6*B*). EGFP-vinculin was detected in tissues expressing WT EGFP-vinculin or vinculin Y1065E, indicating that recombinant vinculin as well as endogenous vincu-

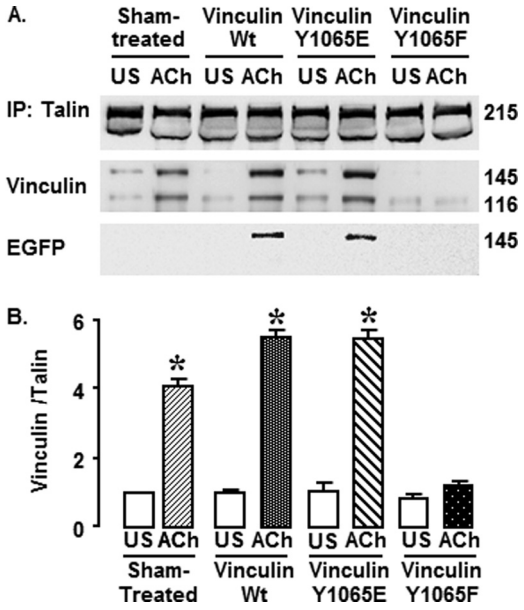

FIGURE 6. **Expression of vinculin Y1065F mutant protein decreases the interaction between vinculin and talin in tracheal smooth muscle tissues.** Talin was immunoprecipitated (*IP*) from tissues expressing WT vinculin, vinculin Y1065E, vinculin Y1065F, or sham-treated tissues after 5 min of stimulation with 10^{-4} M ACh or without stimulation (*US*). *A*, representative immunoblots against talin, vinculin and EGFP from muscle extracts from a single experiment. Endogenous metavinculin and EGFP vinculin both migrate at about 145 kDa, whereas endogenous vinculin migrates at 116 kDa. *B*, relative levels of vinculin that co-precipitated with talin for each treatment group. In ACh-stimulated sham-treated tissues and tissues expressing WT vinculin or vinculin Y1065E more vinculin co-precipitated with talin than in unstimulated tissues. In Y1065F-treated tissues stimulated with ACh, the amount of vinculin that co-precipitated with talin in response to ACh did not increase significantly. *, significant difference between ACh and unstimulated tissues ($n = 4$, $p < 0.05$). *Error bars*, S.E.

lin/metavinculin bind to talin after stimulation with ACh. There were no significant differences in the amount of vinculin that coprecipitated with talin in unstimulated muscles.

We also performed PLAs on freshly dissociated tracheal smooth muscle cells to evaluate the effect of vinculin phosphorylation on the interaction of vinculin with talin and to determine the localization of vinculin/talin protein complexes (Fig. 7, *A* and *B*). In unstimulated cells, few PLA fluorescent spots were observed in any of the cells indicating little interaction between talin and vinculin (Fig. 7*A*). Stimulation with ACh triggered the interaction of vinculin with talin at the membrane in sham-treated and vinculin Y1065E-expressing cells, as evidenced by fluorescent spots along the cell membrane. In contrast, ACh stimulation elicited few interactions between vinculin and talin in cells expressing vinculin Y1065F. These results demonstrate that vinculin phosphorylation at tyrosine 1065 in response to stimulation with ACh is needed for vinculin and talin to interact at the cell membrane. Taken in sum, the results shown in Figs. 5–7 suggest that phosphorylation-deficient vinculin Y1065F is recruited to the smooth muscle cell membrane in response to stimulation with ACh but that it cannot interact with talin.

Phosphorylation at Tyr[1065] Promotes the Open Conformation of Vinculin (Fig. 8)—Vinculin WT, Y1065E, and Y1065F conformation-sensitive FRET probes were expressed in tracheal smooth muscle tissues to determine whether vinculin phosphorylation at Tyr^{1065} contributes to regulation of vinculin conformation. The effect of phosphorylation at Tyr^{1065} on vinculin conformation was first analyzed in extracts of tissues expressing the conformation-sensitive FRET probes (Fig. 8*A*). For each treatment group, tissues were stimulated with 10^{-5} M ACh for 5 min or left unstimulated, and then they were rapidly frozen. The donor/acceptor emission ratio from tissues expressing WT vinculin conformation-sensitive FRET probes was significantly higher in ACh-stimulated tissues than in unstimulated tissues, indicating that stimulation with ACh results in the conversion of vinculin to an open conformation (Fig. 8*A*). The phosphomimetic vinculin Y1065E FRET probe also maintained a closed conformation in unstimulated tissues, but the donor/emission ratio significantly increased after stimulation with ACh, indicating conversion of vinculin to an open conformation (Fig. 8*A*) ($p < 0.05$). In contrast, in tissues expressing the non-phosphorylatable vinculin Y1065F FRET probes, stimulation with ACh did not increase the donor/acceptor emission ratio, indicating that the vinculin Y1065F FRET probe remained in a closed conformation.

The effect of Tyr^{1065} phosphorylation on the molecular conformation of vinculin was also evaluated in cells freshly dissociated from tissues expressing the conformation-sensitive vinculin FRET probes (Fig. 8*B*). Freshly dissociated cells were stimulated with ACh 10 min after plating them onto coverslips, and spectral confocal microscopy was used to evaluate fluorescence emissions at 470 and 530 nm. In dissociated smooth muscle cells expressing vinculin WT and vinculin Y1065E, stimulation with ACh induced the conversion of vinculin to an open conformation, whereas in cells expressing vinculin Y1065F, stimulation with ACh did not provoke a shift in the conformation of vinculin to the activated state. There were no differences in the conformation of vinculin in unstimulated cells expressing WT, Y1065E, or Y1065F FRET probes. These observations were similar to those in the tissue extracts, confirming that the process of cell dissociation and plating onto coverslips did not significantly alter the conformation status of vinculin.

Activated Vinculin Localizes to the Cortex of Smooth Muscle Cells (Fig. 9)—We evaluated the cellular localization of the WT, Y1065E, and Y1065F vinculin conformation-sensitive FRET probes in live cells by comparing fluorescence emissions in regions just inside the plasma membrane with central cytoplasmic regions of each cell (Fig. 9*A*). The total fluorescence emission of the probes over the entire spectrum from 420 to 660 nm was calculated for each region, and the mean fluorescence intensity of membrane regions and cytoplasmic regions was separately determined (Fig. 9*B*). In cells expressing vinculin WT, Y1065E, and Y1065F conformation-sensitive FRET probes, ACh stimulation caused similar increases in fluorescence intensity at the submembranous cell cortex; there were no significant differences in the ratio of membrane to cytoplasmic fluorescence in ACh-stimulated or unstimulated cells expressing the different vinculin Tyr^{1065} phosphorylation mutants ($p > 0.05$) (Fig. 9*B*). These results indicate that phosphorylation at Tyr^{1065} is not required for the recruitment of vinculin conformation-sensitive FRET probes to cell membrane in response to ACh and are consistent with the data from live cells showing that recruitment of EGFP vinculin was also

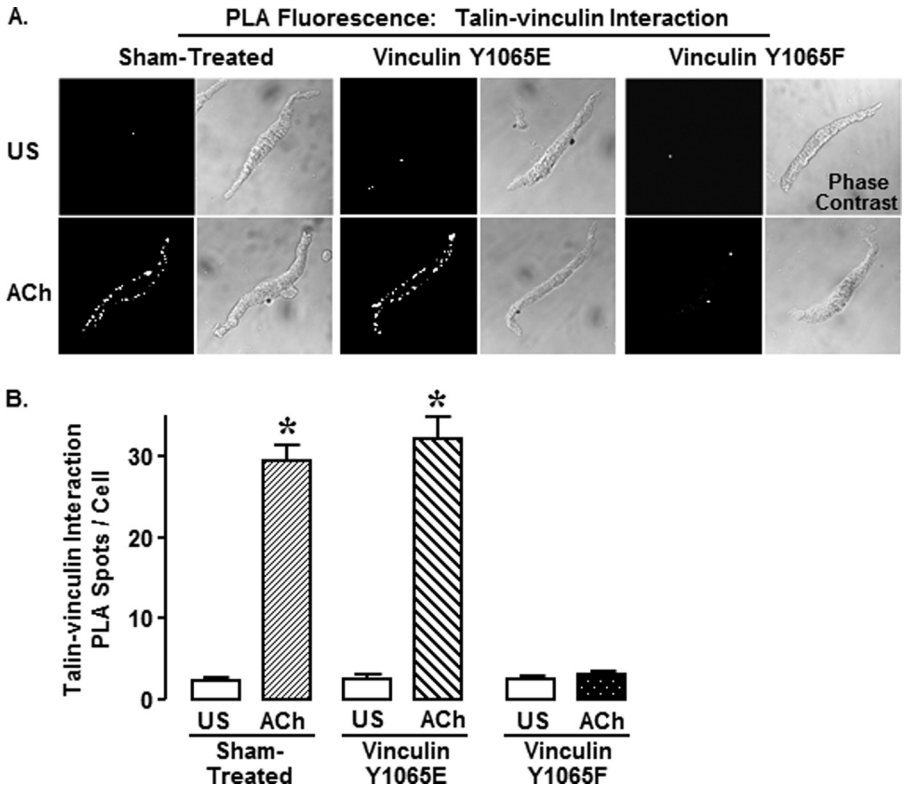

FIGURE 7. **Expression of vinculin Y1065F in tracheal smooth muscle tissues inhibited the ACh-stimulated increase in the interaction between vinculin and talin, as detected by *in situ* PLAs performed on freshly dissociated cells.** *A*, fluorescence and phase-contrast images of unstimulated (*US*) and ACh-stimulated smooth muscle cells from tissues expressing vinculin Y1065E or vinculin Y1065F or sham-treated. Each fluorescent spot (PLA spot) indicates interaction between talin and vinculin. *B*, the number of PLA spots was significantly higher in ACh-stimulated smooth muscle cells than in unstimulated cells in sham-treated tissues (unstimulated, $n = 44$; ACh, $n = 59$) and tissues expressing vinculin Y1065E (unstimulated, $n = 34$; ACh, $n = 40$). ACh did not stimulate an increase in vinculin-talin interactions in cells dissociated from tissues expressing vinculin Y1065F (unstimulated, $n = 40$; ACh, $n = 42$). All of the values are the means ± S.E. (*error bars*). *, significant difference between ACh and unstimulated cells ($p < 0.05$).

unaffected by mutations at the Tyr^{1065} phosphorylation site (Fig. 5).

The cellular localization of vinculin in closed and open conformations was evaluated in unstimulated and ACh-stimulated cells dissociated from tissues expressing the vinculin WT, Y1065F, or Y1065E conformation-sensitive probes. In the cells from vinculin WT-transfected tissues (Fig. 10*A*), the ratio of donor emission/acceptor emission was significantly higher at cell membrane than in the central cytoplasm in both unstimulated and ACh-stimulated cells. Thus, regardless of the stimulation status of the cells, a majority of conformation-sensitive WT vinculin FRET probes in the submembranous cortical region of the cells remain in an open conformation, and the majority of WT probes in the cytoplasm remain in a closed conformation.

In cells from tissues expressing phosphomimetic vinculin Y1065E conformation-sensitive probes, the localization of vinculin in the open and closed conformations was similar to that of the WT probes. In both stimulated and unstimulated cells, the majority of vinculin Y1065E FRET probes maintained an open conformation at the cell cortex and a closed conformation in the cytoplasm (Fig. 10*B*). This finding indicates that the phosphorylation of vinculin at Tyr^{1065} does not by itself trigger the conversion of vinculin to an open conformation or the recruitment of vinculin to the cell cortex.

In cells from tissues expressing the nonphosphorylatable vinculin Y1065F conformation-sensitive probes, the ratio of donor/acceptor emission was low both at the cell membrane and in the cytoplasm in both unstimulated and ACh-stimulated cells (Fig. 10*C*). This indicates that vinculin Y1065F maintains a closed conformation at the cell membrane and in the cytoplasm in both unstimulated and stimulated cells. Thus, the vinculin probes that cannot be phosphorylated at Tyr^{1065} are recruited to the membrane in response to stimulation with ACh, but they do not maintain an open conformation, and thus the scaffolding function of vinculin is absent.

In summary, these data show that stimulation with ACh triggers the recruitment of vinculin FRET probes to the cell membrane regardless of their phosphorylation status. However, after localization to the membrane, the vinculin must undergo tyrosine phosphorylation in order to maintain an open conformation and interact with talin.

DISCUSSION

Our results provide the first demonstration that the phosphorylation of Tyr^{1065} on the C terminus of the vinculin molecule is a critical step in the regulation of its molecular conformation and scaffolding function and that vinculin phosphorylation at this site is a prerequisite for the generation of contractile tension by smooth muscle cells and tissues in response to a contractile stimulus. We found that conformation-sensitive vinculin FRET probes expressed in smooth muscle tissues undergo conversion from an autoinhibited "closed" conformation to an open "activated" conformation at the mem-

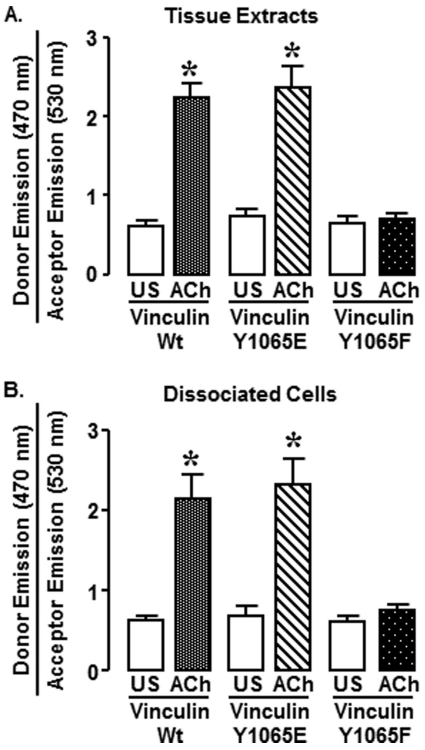

FIGURE 8. **Non-phosphorylatable vinculin Y1065F FRET probes do not convert to an open conformation in response to ACh in smooth muscle tissues and cells.** *A*, fluorescence emissions at 470 nm (donor) and 530 nm (acceptor) in extracts from smooth muscle tissues were measured using a MicroSpectrometer after excitation at 405 nm. The donor/acceptor emission ratio was significantly higher in tissues expressing the vinculin WT or Y1065E FRET probes, but the donor/acceptor emission ratio was not increased in tissues expressing the Y1065F FRET probe. *, significant difference between ACh and unstimulated (*US*) tissues ($n = 4–5$, $p < 0.05$). *B*, ratio of donor (470 nm)/acceptor (530 nm) emission was measured in dissociated smooth muscle cells using an Olympus FV1000-MPE spectral confocal microscope. The donor/acceptor emission ratio was significantly higher in ACh-stimulated cells from tissues expressing the vinculin WT FRET probe (unstimulated, $n = 8$; ACh, $n = 6$) or Y1065E FRET probe (unstimulated, $n = 6$; ACh, $n = 4$). ACh stimulation did not increase the donor/acceptor emissions ratio in cells from tissues expressing the vinculin Y1065F FRET probe (unstimulated, $n = 7$; ACh, $n = 19$). *, significant difference between ACh and unstimulated cells ($p < 0.05$). *Error bars*, S.E.

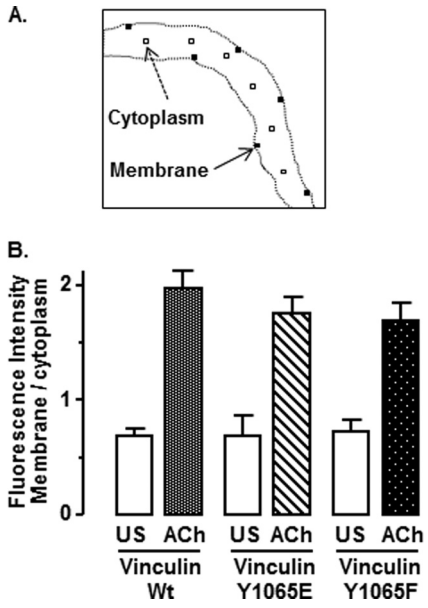

FIGURE 9. **Phosphorylation at Tyr[1065] does not affect the recruitment of vinculin FRET probes to the membrane in response to ACh.** *A*, the average fluorescence intensity at the plasma membrane and in the central cytoplasmic regions of cells dissociated from smooth muscle tissues expressing vinculin FRET probes was analyzed by averaging emissions in six 1-μm^2 regions along the membrane and six 1-μm^2 regions in the cytoplasm. *B*, to determine the cellular localization of the FRET probes, the total fluorescence emission of the probes over the entire spectrum from 420 to 660 nm was calculated for each region, and the mean fluorescence intensities of membrane regions and cytoplasmic regions were separately determined. In unstimulated cells (*US*), the ratio of fluorescence intensity of membrane/cytoplasm was less than 1 in all groups of cells. Stimulation with ACh significantly increased the fluorescence intensity at the cell membrane in all groups of cells, regardless of the phosphorylation status of the vinculin FRET probe. There were no significant differences in the ratio of fluorescence intensity of membrane/cytoplasm among ACh-stimulated or unstimulated cells expressing the different vinculin Tyr[1065] phosphorylation mutant FRET probes ($p > 0.05$). Values are mean ± S.E. (*error bars*): vinculin WT (unstimulated, $n = 7$; ACh, $n = 7$), vinculin Y1065E (unstimulated, $n = 3$; ACh, $n = 5$), vinculin Y1065F (unstimulated, $n = 7$; ACh, $n = 16$).

brane of the smooth muscle cell in response to the contractile stimulation and that this conformational shift requires vinculin phosphorylation at the Tyr[1065] site. In its open conformation, vinculin provides a scaffold for the binding of talin and actin at integrin adhesion sites in the smooth muscle cell and can thus mediate the transmission of contractile tension from the cytoskeleton to the extracellular matrix. Our results show that tension development in smooth muscle depends on the regulated assembly and fortification of membrane adhesome complexes by vinculin and that external stimuli can regulate this process by regulating the phosphorylation of vinculin.

We have previously shown that contractile stimulation triggers the recruitment of vinculin to the membrane of tracheal smooth muscle cells, where it binds to talin, and that the recruitment of vinculin to membrane adhesomes is necessary for normal tension development in tracheal smooth muscle tissues (10, 23). In the present study, we used EGFP vinculin with point mutations at the tyrosine 1065 site (phosphomimetic vinculin-vinculin Y1065E and non-phosphorylatable vinculin-vinculin Y1065F) to analyze the role of vinculin phosphorylation at Tyr[1065] in the regulation of its recruitment to the membrane. Stimulation with ACh triggered the membrane recruitment of the non-phosphorylatable and the constitutively phosphorylated vinculin Tyr[1065] site mutants as well as wild type EGFP vinculin proteins, regardless of their phosphorylation status. Vinculin Y1065F and Y1065E FRET probes were also recruited to the membrane in response to stimulation of smooth muscle cells with ACh (Fig. 10, *A–C*). Analysis of emissions from the wild type vinculin and vinculin Y1065E FRET probes showed that they converted to an open activated conformation after being recruited to the membrane, whereas the non-phosphorylatable vinculin Y1065F FRET probes remained localized at the membrane in a closed autoinhibited conformation. Thus, the recruitment of vinculin to the membrane does not require Tyr[1065] phosphorylation; phosphorylation and conversion to an open conformation occur after vinculin localizes to the membrane. Previous analysis using vinculin FRET probes in mouse embryo cells has shown that the conformation of vinculin and its recruitment to the membrane can be uncoupled (46).

Our results clearly show that vinculin phosphorylation regulates its ability to interact with talin. The binding of talin and vinculin was detected in freshly dissociated airway smooth muscle cells using proximity ligation assays. Few interactions

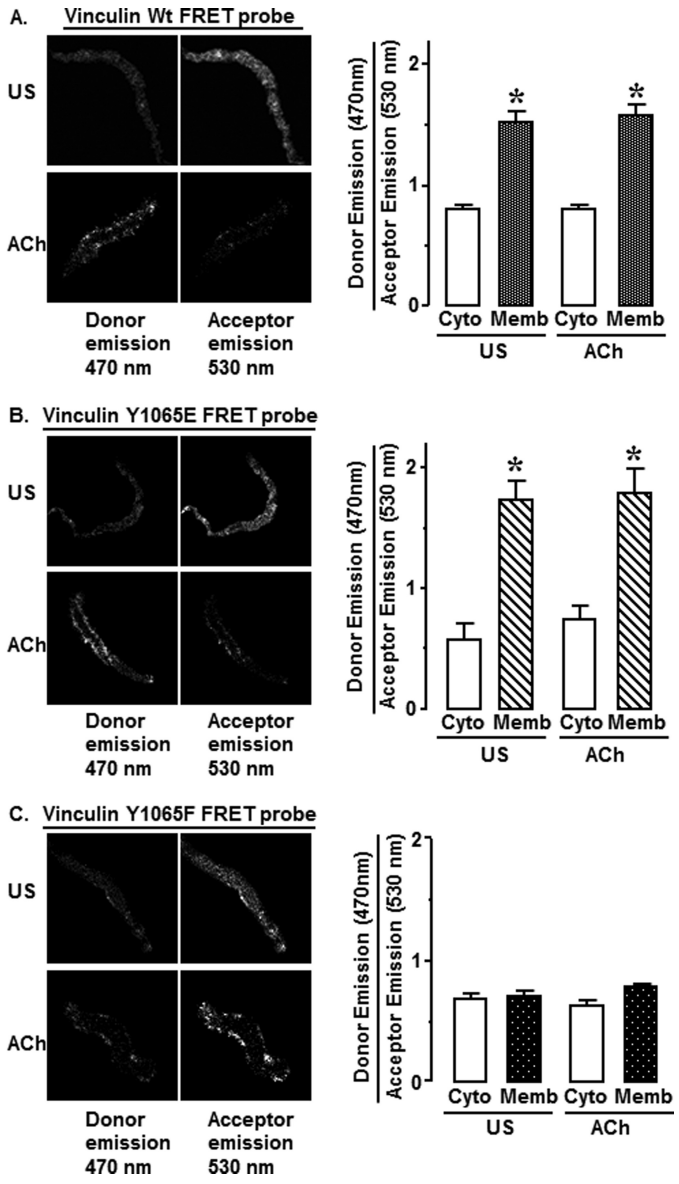

FIGURE 10. **Tyr[1065] phosphorylation is required for vinculin to assume an open conformation in dissociated smooth muscle cells.** Shown are fluorescence images at 470 nm (donor) and 530 nm (acceptor) emissions from unstimulated (*US*) and ACh-stimulated cells dissociated from tissues expressing vinculin WT, 1065E, or 1065F FRET probes. An increase in donor emissions indicates that more vinculin is in an open conformation. *A*, WT vinculin FRET probes maintain an open conformation at the cell membrane and a closed conformation in the cytoplasm. Mean ratios of donor emission (470 nm)/acceptor emission (530 nm) from cells expressing vinculin FRET WT probes were higher at membrane regions than that in cytoplasm in both unstimulated and ACh-stimulated cells (unstimulated, $n = 7$; ACh, $n = 8$). *B*, vinculin phosphomimetic Y1065E FRET probes maintain an open conformation at the cell membrane and a closed conformation in the cytoplasm. ACh stimulation increased fluorescence intensity at 470 nm. Mean ratios of donor emission (470 nm)/acceptor emission (530 nm) from cells expressing vinculin Y1065E FRET probes were higher at membrane regions than that in cytoplasm (unstimulated, $n = 3$; ACh, $n = 5$). *C*, vinculin non-phosphorylatable Y1065F FRET probes maintain a closed conformation at the cell membrane and in the cytoplasm. ACh stimulation did not cause an increase in fluorescence intensity at 470 nm. No significant difference was detected in the ratio of donor emission (470 nm)/acceptor emission (530 nm) at the membrane regions or in the cytoplasm (unstimulated, $n = 7$; ACh, $n = 16$). *, significant difference between membrane and cytoplasm ($p < 0.05$). *Error bars*, S.E.

between vinculin and talin were observed in unstimulated cells regardless of the phosphorylation status of vinculin, but ACh stimulation resulted in a dramatic increase in the formation of vinculin-talin complexes at the membrane of cells expressing wild type vinculin or constitutively phosphorylated vinculin (vinculin Y1065E). However, expression of the phosphorylation-deficient vinculin (Y1065F) prevented the formation of vinculin-talin complexes in response to stimulation with ACh. All of the vinculin-talin complexes were observed at the membrane; none were in the cytoplasm under any conditions. Similar results were obtained by co-immunoprecipitation of vinculin and talin from extracts of intact muscle tissues, confirming that our results were not a function of the isolation or plating of the smooth muscle cells onto an artificial substrate. Our results show that the recruitment of vinculin to membrane adhesomes triggered by a contractile stimulus and the conversion of vinculin to its active open conformation are distinct and independently regulated events, with only the activation step dependent on Tyr[1065] phosphorylation.

We previously found that vinculin maintains a stable complex with paxillin in tracheal smooth muscle regardless of its activation state, and the membrane recruitment of the vinculin-paxillin complex requires the presence of the focal adhesion targeting domain of the paxillin molecule (10, 23). Our present observation that inactive closed vinculin can be recruited to the membrane in response to external stimulation is consistent with our previous findings that the targeting of vinculin to the membrane depends on paxillin (Figs. 9 and 10). After localization to the adhesome, vinculin requires Tyr[1065] phosphorylation to maintain an active conformation in which it can bind to talin and other ligands. Thus, the recruitment of vinculin to adhesome sites alone is clearly not sufficient for normal tension development; the conversion of vinculin to an activated ligand-binding conformation is also required.

Previous investigators have suggested that vinculin phosphorylation at Tyr[1065] may contribute to the regulation of its conformation (37, 48). Although vinculin has long been recognized as a tyrosine phosphorylation substrate (49), Zhang *et al.* (37) were the first to map one of the phosphorylation sites to Tyr[1065] near the C terminus of the molecule within the tail domain and to demonstrate that phosphorylation at this site, as well as at Tyr[100], affects cell spreading in activated platelets. They also used pull-down assays to analyze the effect of Tyr[1065] phosphorylation on the affinity of vinculin tail domain fragments for the head domain and found that the phosphorylation markedly reduced the affinity of the tail domain for the head domain. Structural modeling analysis by Golji *et al.* (48) also suggested that phosphorylation on Tyr[1065] would reduce the strength of the vinculin head-tail interaction and make vinculin more susceptible to activation by its ligands. Our results using the phosphorylation deficient vinculin FRET probe (vinculin Y1065F) demonstrate that the activated conformation of vinculin cannot be maintained in living smooth muscle cells in the absence of its phosphorylation at Tyr[1065], even in vinculin molecules residing at the cell cortex. In contrast, constitutively phosphorylated vinculin mutants in the cytoplasm remain in an inactive conformation until they are recruited to the membrane, demonstrating that Tyr[1065] phosphorylation of vinculin is not by

itself sufficient to trigger a change in the conformation of vinculin. Thus, under physiologic conditions, phosphorylation at Tyr^{1065} is a necessary but not a sufficient step in the activation of vinculin to an open conformation.

The function of vinculin phosphorylation at Tyr^{1065} has been previously investigated in cultured migrating human epidermal keratinocytes and a mouse embryonic fibroblast cell line using vinculin phosphorylation site mutants (39, 40, 50). In the kerotinocytes, vinculin phosphorylation at Tyr^{1065} was transient and was correlated with increased vinculin exchange dynamics during focal adhesion growth (39). Focal adhesion maturation was correlated with a reduction in vinculin phosphorylation and associated with an increase in cellular adhesive traction force. In the embryonic fibroblasts, the expression of vinculin 1065F mutants inhibited vinculin exchange dynamics and reduced substrate adhesive traction force (40, 50). The authors speculated that an increase in vinculin phosphorylation was necessary for its incorporation into focal adhesions but that the dephosphorylation of vinculin after its incorporation is necessary for the development of stable adhesion junctions and for an increase in traction force.

In contrast, we found that phosphorylated vinculin remains stably localized at cell adhesion junctions in smooth muscle and that vinculin phosphorylation remains elevated for the duration of contraction. Active tension generated by smooth muscle tissues was markedly suppressed when vinculin phosphorylation was inhibited despite the sustained localization of vinculin at adhesion junctions. Our results show that stably localized vinculin cannot maintain an open active conformation without phosphorylation at Tyr^{1065}. Our results suggest that the dynamics of vinculin exchange and phosphorylation differ in differentiated smooth muscle cells from that in migrating cells or cultured cells that are in the process of substrate adhesion.

The response of smooth muscle cells to a contractile stimulus depends on the integration of signals from the environment with those initiated by neural and hormonal stimuli. Proteins within adhesome complexes are strategically localized to sense extracellular signals, such as mechanical stress or changes in matrix proteins, and transduce them to cytoskeletal signaling pathways that interact with those initiated by the activation of hormonal receptors. Vinculin plays a key role in this process by providing a scaffold for the assembly of adhesome complexes that regulate cytoskeletal signaling pathways. Our results demonstrate that in smooth muscle, contractile stimuli actively regulate the scaffolding function of vinculin by stimulating the phosphorylation of vinculin and that the Tyr^{1065} site is a critical phosphorylation site in the regulation of the conformation of the vinculin molecule.

REFERENCES

1. Saito, S. Y., Hori, M., Ozaki, H., and Karaki, H. (1996) Cytochalasin D inhibits smooth muscle contraction by directly inhibiting contractile apparatus. *J. Smooth Muscle Res.* **32,** 51–60
2. Mehta, D., and Gunst, S. J. (1999) Actin polymerization stimulated by contractile activation regulates force development in canine tracheal smooth muscle. *J. Physiol.* **519,** 829–840
3. Cipolla, M. J., Gokina, N. I., and Osol, G. (2002) Pressure-induced actin polymerization in vascular smooth muscle as a mechanism underlying myogenic behavior. *FASEB J.* **16,** 72–76
4. Zhang, W., Wu, Y., Du, L., Tang, D. D., and Gunst, S. J. (2005) Activation of the Arp2/3 complex by N-WASp is required for actin polymerization and contraction in smooth muscle. *Am. J. Physiol. Cell Physiol.* **288,** C1145–C1160
5. Chen, X., Pavlish, K., Zhang, H. Y., and Benoit, J. N. (2006) Effects of chronic portal hypertension on agonist-induced actin polymerization in small mesenteric arteries. *Am. J. Physiol. Heart Circ. Physiol.* **290,** H1915–H1921
6. Rembold, C. M., Tejani, A. D., Ripley, M. L., and Han, S. (2007) Paxillin phosphorylation, actin polymerization, noise temperature, and the sustained phase of swine carotid artery contraction. *Am. J. Physiol. Cell Physiol.* **293,** C993–C1002
7. Gunst, S. J., and Zhang, W. (2008) Actin cytoskeletal dynamics in smooth muscle. A new paradigm for the regulation of smooth muscle contraction. *Am. J. Physiol. Cell Physiol.* **295,** C576–C587
8. Kim, H. R., Gallant, C., Leavis, P. C., Gunst, S. J., and Morgan, K. G. (2008) Cytoskeletal remodeling in differentiated vascular smooth muscle is actin isoform-dependent and stimulus-dependent. *Am. J. Physiol. Cell Physiol.* **295,** C768–C778
9. Zhang, W., Du, L., and Gunst, S. J. (2010) The effects of the small GTPase RhoA on the muscarinic contraction of airway smooth muscle result from its role in regulating actin polymerization. *Am. J. Physiol. Cell Physiol.* **299,** C298–C306
10. Huang, Y., Zhang, W., and Gunst, S. J. (2011) Activation of vinculin induced by cholinergic stimulation regulates contraction of tracheal smooth muscle tissue. *J. Biol. Chem.* **286,** 3630–3644
11. North, A. J., Galazkiewicz, B., Byers, T. J., Glenney, J. R., Jr., and Small, J. V. (1993) Complementary distributions of vinculin and dystrophin define two distinct sarcolemma domains in smooth muscle. *J. Cell Biol.* **120,** 1159–1167
12. Geiger, B., Dutton, A. H., Tokuyasu, K. T., and Singer, S. J. (1981) Immunoelectron microscope studies of membrane-microfilament interactions. Distributions of α-actinin, tropomyosin, and vinculin in intestinal epithelial brush border and chicken gizzard smooth muscle cells. *J. Cell Biol.* **91,** 614–628
13. Burridge, K., Fath, K., Kelly, T., Nuckolls, G., and Turner, C. (1988) Focal adhesions. Transmembrane junctions between the extracellular matrix and the cytoskeleton. *Annu. Rev. Cell Biol.* **4,** 487–525
14. Johnson, R. P., and Craig, S. W. (1994) An intramolecular association between the head and tail domains of vinculin modulates talin binding. *J. Biol. Chem.* **269,** 12611–12619
15. Bois, P. R., Borgon, R. A., Vonrhein, C., and Izard, T. (2005) Structural dynamics of α-actinin-vinculin interactions. *Mol. Cell Biol.* **25,** 6112–6122
16. Bass, M. D., Smith, B. J., Prigent, S. A., and Critchley, D. R. (1999) Talin contains three similar vinculin-binding sites predicted to form an amphipathic helix. *Biochem. J.* **341,** 257–263
17. Bubeck, P., Pistor, S., Wehland, J., and Jockusch, B. M. (1997) Ligand recruitment by vinculin domains in transfected cells. *J. Cell Sci.* **110,** 1361–1371
18. Cohen, D. M., Kutscher, B., Chen, H., Murphy, D. B., and Craig, S. W. (2006) A conformational switch in vinculin drives formation and dynamics of a talin-vinculin complex at focal adhesions. *J. Biol. Chem.* **281,** 16006–16015
19. Johnson, R. P., and Craig, S. W. (1995) F-actin binding site masked by the intramolecular association of vinculin head and tail domains. *Nature* **373,** 261–264
20. Small, J. V. (1985) Geometry of actin-membrane attachments in the smooth muscle cell. The localizations of vinculin and α-actinin. *EMBO J.* **4,** 45–49
21. Eddinger, T. J., Schiebout, J. D., and Swartz, D. R. (2005) Smooth muscle adherens junctions associated proteins are stable at the cell periphery during relaxation and activation. *Am. J. Physiol. Cell Physiol.* **289,** C1379–C1387
22. DeMali, K. A., and Burridge, K. (2003) Coupling membrane protrusion and cell adhesion. *J. Cell Sci.* **116,** 2389–2397
23. Opazo Saez A., Zhang, W., Wu, Y., Turner, C. E., Tang, D. D., and Gunst,

S. J. (2004) Tension development during contractile stimulation of smooth muscle requires recruitment of paxillin and vinculin to the membrane. *Am. J. Physiol. Cell Physiol.* **286,** C433–C447
24. Zhang, W., Huang, Y., and Gunst, S. J. (2012) The small GTPase RhoA regulates the contraction of smooth muscle tissues by catalyzing the assembly of cytoskeletal signaling complexes at membrane adhesion sites. *J. Biol. Chem.* **287,** 33996–34008
25. Bakolitsa, C., Cohen, D. M., Bankston, L. A., Bobkov, A. A., Cadwell, G. W., Jennings, L., Critchley, D. R., Craig, S. W., and Liddington, R. C. (2004) Structural basis for vinculin activation at sites of cell adhesion. *Nature* **430,** 583–586
26. Ziegler, W. H., Liddington, R. C., and Critchley, D. R. (2006) The structure and regulation of vinculin. *Trends Cell Biol.* **16,** 453–460
27. Izard, T., Evans, G., Borgon, R. A., Rush, C. L., Bricogne, G., and Bois, P. R. (2004) Vinculin activation by talin through helical bundle conversion. *Nature* **427,** 171–175
28. Chen, H., Choudhury, D. M., and Craig, S. W. (2006) Coincidence of actin filaments and talin is required to activate vinculin. *J. Biol. Chem.* **281,** 40389–40398
29. Bois, P. R., O'Hara, B. P., Nietlispach, D., Kirkpatrick, J., and Izard, T. (2006) The vinculin binding sites of talin and α-actinin are sufficient to activate vinculin. *J. Biol. Chem.* **281,** 7228–7236
30. Izard, T., and Vonrhein, C. (2004) Structural basis for amplifying vinculin activation by talin. *J. Biol. Chem.* **279,** 27667–27678
31. Golji, J., and Mofrad, M. R. (2010) A molecular dynamics investigation of vinculin activation. *Biophys. J.* **99,** 1073–1081
32. Golji, J., Lam, J., and Mofrad, M. R. (2011) Vinculin activation is necessary for complete talin binding. *Biophys. J.* **100,** 332–340
33. Palmer, S. M., Playford, M. P., Craig, S. W., Schaller, M. D., and Campbell, S. L. (2009) Lipid binding to the tail domain of vinculin. Specificity and the role of the N and C termini. *J. Biol. Chem.* **284,** 7223–7231
34. Weekes, J., Barry, S. T., and Critchley, D. R. (1996) Acidic phospholipids inhibit the intramolecular association between the N- and C-terminal regions of vinculin, exposing actin-binding and protein kinase C phosphorylation sites. *Biochem. J.* **314,** 827–832
35. Gilmore, A. P., and Burridge, K. (1996) Regulation of vinculin binding to talin and actin by phosphatidyl-inositol-4-5-bisphosphate. *Nature* **381,** 531–535
36. Dumbauld, D. W., Lee, T. T., Singh, A., Scrimgeour, J., Gersbach, C. A., Zamir, E. A., Fu, J., Chen, C. S., Curtis, J. E., Craig, S. W., and García, A. J. (2013) How vinculin regulates force transmission. *Proc. Natl. Acad. Sci. U.S.A.* **110,** 9788–9793
37. Zhang, Z., Izaguirre, G., Lin, S. Y., Lee, H. Y., Schaefer, E., and Haimovich, B. (2004) The phosphorylation of vinculin on tyrosine residues 100 and 1065, mediated by SRC kinases, affects cell spreading. *Mol. Biol. Cell* **15,** 4234–4247
38. Ziegler, W. H., Tigges, U., Zieseniss, A., and Jockusch, B. M. (2002) A lipid-regulated docking site on vinculin for protein kinase C. *J. Biol. Chem.* **277,** 7396–7404
39. Möhl, C., Kirchgessner, N., Schäfer, C., Küpper, K., Born, S., Diez, G., Goldmann, W. H., Merkel, R., and Hoffmann, B. (2009) Becoming stable and strong. The interplay between vinculin exchange dynamics and adhesion strength during adhesion site maturation. *Cell Motil. Cytoskeleton* **66,** 350–364
40. Küpper, K., Lang, N., Möhl, C., Kirchgessner, N., Born, S., Goldmann, W. H., Merkel, R., and Hoffmann, B. (2010) Tyrosine phosphorylation of vinculin at position 1065 modifies focal adhesion dynamics and cell tractions. *Biochem. Biophys. Res. Commun.* **399,** 560–564
41. Cohen, D. M., Chen, H., Johnson, R. P., Choudhury, B., and Craig, S. W. (2005) Two distinct head-tail interfaces cooperate to suppress activation of vinculin by talin. *J. Biol. Chem.* **280,** 17109–17117
42. Tang, D. D., Turner, C. E., and Gunst, S. J. (2003) Expression of non-phosphorylatable paxillin mutants in canine tracheal smooth muscle inhibits tension development. *J. Physiol.* **553,** 21–35
43. Zhang, W., and Gunst, S. J. (2006) Dynamic association between alpha-actinin and β-integrin regulates contraction of canine tracheal smooth muscle. *J. Physiol.* **572,** 659–676
44. Hathaway, D. R., and Haeberle, J. R. (1985) A radioimmunoblotting method for measuring myosin light chain phosphorylation levels in smooth muscle. *Am. J. Physiol.* **249,** C345–C351
45. Söderberg, O., Gullberg, M., Jarvius, M., Ridderstråle, K., Leuchowius, K. J., Jarvius, J., Wester, K., Hydbring, P., Bahram, F., Larsson, L. G., and Landegren, U. (2006) Direct observation of individual endogenous protein complexes *in situ* by proximity ligation. *Nat. Methods* **3,** 995–1000
46. Chen, H., Cohen, D. M., Choudhury, D. M., Kioka, N., and Craig, S. W. (2005) Spatial distribution and functional significance of activated vinculin in living cells. *J. Cell Biol.* **169,** 459–470
47. Koushik, S. V., Chen, H., Thaler, C., Puhl, H. L., 3rd, and Vogel, S. S. (2006) Cerulean, Venus, and VenusY67C FRET reference standards. *Biophys. J.* **91,** L99-L101
48. Golji, J., Wendorff, T., and Mofrad, M. R. (2012) Phosphorylation Primes Vinculin for Activation. *Biophys. J.* **102,** 2022–2030
49. Sefton, B. M., Hunter, T., Ball, E. H., and Singer, S. J. (1981) Vinculin. A cytoskeletal target of the transforming protein of Rous sarcoma virus. *Cell* **24,** 165–174
50. Diez, G., Kollmannsberger, P., Mierke, C. T., Koch, T. M., Vali, H., Fabry, B., and Goldmann, W. H. (2009) Anchorage of vinculin to lipid membranes influences cell mechanical properties. *Biophys. J.* **97,** 3105–3112